J Intell Robot Syst (2018) 90:253–265
DOI 10.1007/s10846-017-0666-7

Self-Balancing Controlled Lagrangian and Geometric Control of Unmanned Mobile Robots

Morteza Tayefi[1] · **Zhiyong Geng**[1]

Received: 4 December 2016 / Accepted: 25 May 2017 / Published online: 18 September 2017

Abstract This work presents a novel geometric framework for self-balancing as well as planar motion control of wheeled vehicles with two fewer control inputs than the configuration variables. For self-balancing control, we shape the kinetic energy in such a way that the upright direction of the robot's body becomes a nonlinearly stable equilibrium for the corresponding controlled Lagrangian which is inherently a saddle point. Then for planar motion control of the robot, we set its position and attitude as an element of the special Euclidean group SE(2) and apply a logarithmic feedback control taking advantage of the Lie group exponential coordinates. For simulation and evaluating the controllers, the unified dynamic model of the self-balancing mobile robot (SMR) is developed using the constrained Euler-Lagrange equations.

Keywords Nonlinear control · Energy shaping · Lie group · Self-balancing robot · Posture stabilization

1 Introduction

The dynamics of a self-balancing robot is associated with a first-order nonholonomic constraint due to the rolling of the wheels without slipping and a second-order nonholonomic constraint due to the inverted pendulum-like body of the robot. Hence the system is two degrees underactuated, i.e., the four configuration variables including the position components and yaw and pitch angles must be controlled using the only two torque inputs applied to the wheels. Because of this theoretical nature and attractive applications of an SMR, its self-balancing and motion control have recently become an active field of research in robotics and control engineering.

For self-balancing control of wheeled systems, several design methodologies have been investigated in the literature mostly based on the linearized system, see [1] for a review. Some of the approaches which are addressed to solving the problem are as follows: pole placement, PID and LQR controllers, sliding mode control, fuzzy logic controller, adaptive and robust controllers, or a combination of them, see for instance [2–6]. A comparison of controllers for balancing wheeled inverted pendulum robots is presented in [7]. A two-level velocity controller and a stabilizing position controller are derived for a wheeled inverted pendulum using the method of partial feedback linearization in [8]. The paper [9] presents adaptive robust regulation methods for self-balancing and yaw motion of a two-wheeled human transportation vehicle.

Since the SMR is an unmanned vehicle, it must be able to control not only the velocity but also its complete posture (position and orientation) while it is self-balanced at the upright. For this purpose, we first propose the powerful method of controlled Lagrangian(CL) which enables us to reconstruct the robot's nonlinear dynamics such that its stable equilibrium moves above the pivot point from the downward. Note that the stability of the robot's inverted body is valid over large regions of attraction which can compensate big deviations for instance due to the collision with an obstacle. The basic idea of CL method, as an energy shaping technique for underactuated systems, is that we transform by feedback a given Lagrangian system to

✉ Zhiyong Geng
zygeng@pku.edu.cn

[1] The State Key Laboratory for Turbulence and Complex Systems Department of Mechanics and Engineering Science, Peking University, Beijing 100871, China

another closed-loop system with sign-definite energy function for which the desired equilibrium becomes a stable point. Then a dissipative feedback can asymptotically stabilize the system at the new equilibrium point. The method is systematically developed and well established in [10–12].

For planar motion control, a desired goal posture must be reached starting from a given initial posture. Due to Brockett's theorem [13], there is an obstruction to the existence of a smooth and time-invariant stabilizing control for nonholonomic systems. In addition, the linearization for unicycle-type systems around a fixed configuration is not controllable and a linear control cannot achieve posture stabilization. Various types of feedback controls for tracking and stabilization of wheeled systems have been proposed, each one carrying their specific advantages and limitations, see e.g. [14–16]. Different kinematic controllers for path following of wheeled mobile robots are compared in [17]. However, unresolved issues still exist, attracting researchers to contribute new strategies and comparatively improve the control requirements such as globality, smoothness, optimality, simplicity, and etc.

The unique combination of geometric and algebraic properties of Lie groups as well as their recent developments in theory and holonomic applications [18] give a promising direction toward designing controllers for nonholonomic vehicles too. The stabilization of holonomic left-invariant systems on the special Euclidean group SE(3) and its subgroups is studied in [19] where the logarithmic feedback exponentially stabilizes the system at the identity and the corresponding velocity generates a so-called screw motion. It is noted that in general associating the system with some velocity constraints breaks the feasibility of this motion. In this paper the control law is developed in such a way that the corresponding velocity satisfies the nonholonomic constraints due to the rolling of the wheels without slipping. For this purpose, the y-component of the control law is set to be zero and a suitable non-smooth term is added to its yaw-component to compensate the distance between the body x-axis and the corresponding holonomic feedback. Then, the kinematic control is applied to the SMR through a backstepping strategy.

To develop the unified dynamic model of the self-balancing robot, we first show that there is a dynamic equivalence between a two-wheeled robot with two torques on its wheels and a unicycle with one torque on its wheel and the other one on its body in yaw direction. Then, the five degrees of freedom (5DF) equations of motion are developed using Lagrange multipliers approach and constrained Euler-Lagrange (EL) equations. Finally, the controllers for the posture stabilization and self-balancing are applied to this model and their performance is evaluated by numerical simulations. Using robot-like markers, the simulation software is also able to plot out the complete posture of the robot involving its position and orientation which helps to observe the trajectories with attitude.

The rest of paper is outlined as follows: In Section 2, the required notations and preliminaries are introduced. In Section 3, the self-balancing controller is designed using the CL method and reshaping the kinetic energy as well as the mass-inertia matrix. Using exponential coordinates of SE(2), a kinematic controller for the planar motion of the robot is designed in Section 4 and then it is extended for the dynamic system through a backstepping technique. The comprehensive dynamics model and numerical simulations are presented in Section 5. Finally the concluding remarks are stated in Section 6.

2 Preliminaries

A schematic of the self-balancing robot is shown in Fig. 1. The notations and variables used in the following sections are introduced in Table 1. In the remaining of this section, we investigate the control equivalent of the two wheeled robot to a unicycle as well as the controllability of the SMR.

2.1 A Control Equivalence

Consider a two-wheeled mobile robot with $(x, y, \psi, \varphi_1, \varphi_2)$ as its configuration and assume that the balance is maintained by a small castor. Using Lagrange multipliers and constrained EL equations, the dynamics of this system satisfies

$$\begin{aligned} &\mathcal{M}\ddot{\phi} = \tau\,; \\ &\mathcal{M} = \begin{bmatrix} c_1 & c_2 \\ c_2 & c_1 \end{bmatrix},\ \phi = \begin{bmatrix} \varphi_1 \\ \varphi_2 \end{bmatrix},\ \tau = \begin{bmatrix} \tau_1 \\ \tau_2 \end{bmatrix} \\ &c_1 = J_{w2} + \tfrac{r^2}{4}m + \tfrac{r^2}{l^2}J,\ c_2 = \tfrac{r^2}{4}m - \tfrac{r^2}{l^2}J. \end{aligned} \tag{1}$$

The following lemma states that the two torque inputs on the wheels are dynamically equivalent to one torque input

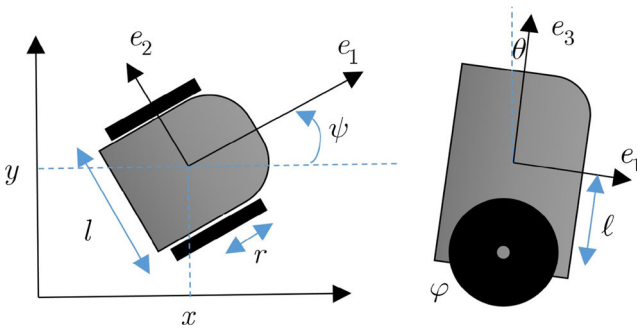

Fig. 1 Schematic of a self-balancing mobile robot in both horizontal and vertical views

Table 1 The notations and system parameters

Symbol	Description
r	Wheel radius
l	Distance between the two wheels
ℓ	Distance between the body center of mass and the pivot point on the wheel axis
x, y	Planar position of the robot in the space (lab.) coordinates, $p = [x, y]^T$
ψ	Yaw angle; the orientation of the robot in the plane
P	Planar posture $P = [\psi, x, y]^T$
g	Lie group element of the planar motion involving ψ, x, y
$\xi, \hat{\xi}$	Lie algebra element of the planar motion
$\eta, \hat{\eta}$	Exponential coordinates of g
θ	Pitch angle; the robot's angle with respect to the vertical
φ_1, φ_2	Rolling angle of the two wheels
φ	Mean value of the two wheels' angles, $\varphi = (\varphi_1 + \varphi_2)/2$
$\mathbf{q}$	Generalized coordinates $\mathbf{q} = [x, y, \psi, \varphi, \theta]^T$
e_1, e_2, e_3	Unit vectors of the body-fixed frame
m_b, J_b	Mass and moment of inertia of the robot's body
m_w, J_w	Mass and moment of inertia of the wheel
J_{bi}, J_{wi}	Component of the moment of inertial about the corresponding $e_i \forall i = 1, 2, 3$
m, J	Mass-inertia parameters, $m = 2m_w + m_b,\ J = J_{w3} + J_{b3}$
h, a, b	System constants, $h = m_b\ell,\ a = J_{w2} + mr^2,\ b = J_{b2} + m_b\ell^2$
τ_1, τ_2	Input torques on the two wheels
u_1, u_2	Unicycle-like control inputs equivalent to the torques τ_1, τ_2

on the wheels' mean angle φ and one torque input on the yaw angle ψ.

Lemma 1 *From a control point of view, the two-wheeled system (1) can be assumed as a unicycle with a torque input on the mean angle φ and a torque input on its yaw angle ψ.*

Proof The nonholonomic constraints due to the rolling without slipping of the wheels implies that

$$\vartheta = \mathcal{D}\dot{\phi}\ ;\ \vartheta = \begin{bmatrix} \dot{\varphi} \\ \dot{\psi} \end{bmatrix},\ \mathcal{D} = \begin{bmatrix} \frac{1}{2} & \frac{1}{2} \\ \frac{r}{l} & \frac{-r}{l} \end{bmatrix} \tag{2}$$

Differentiating (2) and comparing it with Eq. 1 gives

$$\dot{\vartheta} = \mathcal{D}\ddot{\phi} = \mathcal{D}\mathcal{M}^{-1}\tau \tag{3}$$

where

$$\mathcal{D}\mathcal{M}^{-1} = \begin{bmatrix} \frac{1}{2c_3} & \frac{1}{2c_3} \\ \frac{r}{lc_4} & \frac{-r}{lc_4} \end{bmatrix};\ \begin{aligned} c_3 &= c_1 + c_2 = J_{w2} + \tfrac{r^2}{2}m \\ c_4 &= c_1 - c_2 = J_{w2} + \tfrac{2r^2}{l^2}J \end{aligned}$$

The proof now follows by rewriting the above equations as

$$\begin{aligned} c_3\ddot{\varphi} &= \tfrac{1}{2}(\tau_1 + \tau_2) \triangleq u_1 \\ c_4\ddot{\psi} &= \tfrac{r}{l}(\tau_1 - \tau_2) \triangleq u_2 \end{aligned} \tag{4}$$

with the new inputs in φ and ψ directions. □

In this paper, we design the control law for the new input $u = [u_1, u_2]^T$ whereas the wheels' torques can easily be reconstructed by $\tau = \mathcal{D}^{-1}u$. In this framework, the configuration of the two-wheeled system (1) is reduced to the new variables (x, y, ψ, φ). Consequently, the configuration variables or generalized coordinates of the self-balancing robot becomes $\mathbf{q} = [x, y, \psi, \varphi, \theta]^T$.

2.2 Controllability

The Pfaffian form of the velocity constraint due to the nonholonomic constraints yields

$$\begin{bmatrix} 1 & 0 & 0 & -r\cos\psi & 0 \\ 0 & 1 & 0 & -r\sin\psi & 0 \end{bmatrix}\dot{\mathbf{q}} = 0 \tag{5}$$

where the kernel of its coefficient matrix includes

$$f_1 = \begin{bmatrix} 0 \\ 0 \\ 1 \\ 0 \\ 0 \end{bmatrix},\ f_2 = \begin{bmatrix} r\cos\psi \\ r\sin\psi \\ 0 \\ 1 \\ 0 \end{bmatrix},\ f_3 = \begin{bmatrix} 0 \\ 0 \\ 0 \\ 0 \\ 1 \end{bmatrix}.$$

By defining the matrix $G = [f_1, f_2, f_3]$, the velocity constraints (5) forms a kinematic model for the system as

$$\dot{\mathbf{q}} = G\zeta \tag{6}$$

where $\zeta = [\dot{\psi}, \dot{\varphi}, \dot{\theta}]^T$. Since the vector fields f_1, f_2, f_3 are bracket generating, i.e., the Lie brackets

$$[f_1, f_2] = \begin{bmatrix} -r\sin\psi \\ r\cos\psi \\ 0 \\ 0 \\ 0 \end{bmatrix}, \quad [f_1, [f_1, f_2]] = \begin{bmatrix} -r\cos\psi \\ -r\sin\psi \\ 0 \\ 0 \\ 0 \end{bmatrix}$$

generate new directions, according to Frobenius's theorem the system is controllable.

3 Self-Balancing Controlled Lagrangian

For designing the self-balancing control, consider the dynamics in coordinates $q = [\varphi, \theta]^T$. The Lagrangian in this case is

$$L = T - V = \tfrac{1}{2}\dot{q}^T M\dot{q} - V = \tfrac{1}{2}\left(a\dot{\varphi}^2 + 2hr\dot{\varphi}\dot{\theta}\cos\theta + b\dot{\theta}^2\right) - hg\cos\theta \tag{7}$$

with the mass-inertia matrix

$$M = \begin{bmatrix} a & hr\cos\theta \\ hr\cos\theta & b \end{bmatrix}.$$

The corresponding EL equations are now

$$\frac{\mathrm{d}}{\mathrm{d}t}\frac{\partial L}{\partial\dot{\varphi}} = a\ddot{\varphi} + hr\ddot{\theta}\cos\theta - hr\dot{\theta}^2\sin\theta = u_s \tag{8}$$

$$\frac{\mathrm{d}}{\mathrm{d}t}\frac{\partial L}{\partial\dot{\theta}} - \frac{\partial L}{\partial\theta} = b\ddot{\theta} + hr\ddot{\varphi}\cos\theta - hg\sin\theta = -u_s \tag{9}$$

This system is 2DF with the only one control input which appears in both equations. One can easily check that the relative equilibrium $(\theta, \dot{\theta}) = (0, 0)$ corresponding to the upright of the robot's body is an unstable saddle point. The goal is to propose a new mass-inertia matrix such that this equilibrium point becomes stable.

Adapting the notations in [10] enables us to shape the kinetic energy in the following form

$$\begin{aligned} T_c &= \tfrac{1}{2}\dot{q}^T M_c\dot{q} \\ &= \tfrac{1}{2}a\dot{\varphi}^2 + (hr\cos\theta + a\rho)\,\dot{\varphi}\dot{\theta} \\ &\quad + \tfrac{1}{2}\left(b + (\sigma+1)\,a\rho^2 + 2\rho hr\cos\theta\right)\dot{\theta}^2 \end{aligned} \tag{10}$$

with the modified mass-inertia matrix

$$M_c = \begin{bmatrix} a & hr\cos\theta + a\rho \\ hr\cos\theta + a\rho & b + (\sigma+1)\,a\rho^2 + 2\rho hr\cos\theta \end{bmatrix}$$

where ρ is a function of θ and σ is a CL constant, both considered as control parameters to be determined. The geometric procedure to get to this form of kinetic energy by decomposing the tangent space into the horizontal and vertical spaces is explained in [20].

Finding the self-balancing controller follows by the conditions for which the original system in (8) and (9) be equivalent to the one provided by the controlled Lagrangian $L_c = T_c - V$. The new EL equation in φ direction becomes

$$\frac{\mathrm{d}}{\mathrm{d}t}\frac{\partial L_c}{\partial\dot{\varphi}} = a\ddot{\varphi} + hr\ddot{\theta}\cos\theta - hr\dot{\theta}^2\sin\theta + a\rho'\dot{\theta}^2 + a\rho\ddot{\theta} = 0 \tag{11}$$

where $\rho' = d\rho/d\theta$. Comparing (8) and (11) yields the control law as

$$u_c = -a\rho'\dot{\theta}^2 - a\rho\ddot{\theta}. \tag{12}$$

The design procedure follows by specifying the unidentified terms ρ', ρ, and $\ddot{\theta}$. Adding (8) and (9) gives

$$(a + hr\cos\theta)\,\ddot{\varphi} + (b + hr\cos\theta)\,\ddot{\theta} - hr\dot{\theta}^2\sin\theta - hg\sin\theta = 0$$

and substituting $\ddot{\varphi}$ from Eq. 11, we obtain

$$\begin{aligned} &\left(b - (a + hr\cos\theta)\,\rho - a^{-1}h^2r^2\cos^2\theta\right)\ddot{\theta} - hg\sin\theta \\ &+ \left(a^{-1}h^2r^2\sin\theta\cos\theta - \rho'\,(a + hr\cos\theta)\right)\dot{\theta}^2 = 0 \end{aligned} \tag{13}$$

On the other hand, the controlled EL equation corresponding to θ can be written as

$$\begin{aligned} \frac{\mathrm{d}}{\mathrm{d}t}\frac{\partial L_c}{\partial\dot{\theta}} - \frac{\partial L_c}{\partial\theta} &= \left(b + \sigma a\rho^2 - a^{-1}h^2r^2\cos^2\theta\right)\ddot{\theta} \\ &+ \left(a^{-1}h^2r^2\sin\theta\cos\theta + \sigma a\rho\rho'\right)\dot{\theta}^2 \\ &- hg\sin\theta = 0 \end{aligned} \tag{14}$$

where $\ddot{\varphi}$ in the above equation is also substituted from Eq. 11. Comparing (13) and (14) gives

$$(\sigma a\rho + a + hr\cos\theta)\left(\rho\ddot{\theta} + \rho'\dot{\theta}^2\right) = 0.$$

Let the first term be zero, so

$$\rho = -\sigma^{-1}\left(1 + a^{-1}hr\cos\theta\right), \quad \rho' = \sigma^{-1}a^{-1}hr\sin\theta,$$

and $\ddot{\theta}$ can be derived from Eq. 14 by plugging ρ and ρ'. By identifying all the unknown terms ρ, ρ' and $\ddot{\theta}$ in Eq. 12, we get to the following applicable expression of the control input

$$u_c = \frac{\sigma^{-1}\sin\theta\left(hg\,(a + hr\cos\theta) - (b + hr\cos\theta)\,hr\dot{\theta}^2\right)}{b + \sigma^{-1}a\left(1 + a^{-1}hr\cos\theta\right)^2 - a^{-1}h^2r^2\cos^2\theta} \tag{15}$$

In the following proposition, the control parameter σ is specified by the stability analysis of the new Lagrangian dynamics.

Proposition 1 *There always exists a suitable value of the CL constant σ for which the upright of the robot's body, $(\theta, \dot{\theta}) = (0, 0)$, is a stable point for the CL dynamics in* Eqs. 11 and 14 *or equivalently for the EL dynamics in* Eqs. 8 and 9 *with the control input* (15).

Proof The momentum conjugate to φ,

$$\mathrm{J}_\varphi = \frac{\partial L_c}{\partial \dot{\varphi}} = a\dot{\varphi} + (a\rho + hr\cos\theta)\,\dot{\theta},$$

is conserved and is negligible in the process of stability analysis. By this fact, the total shaped energy for the system can be written as

$$E_c = T_c + V = \tfrac{1}{2}a^{-1}\mathrm{J}_\varphi^2 + \tfrac{1}{2}\left(b - a^{-1}h^2r^2\cos^2\theta + \sigma a\rho^2\right)\dot{\theta}^2 + hg\cos\theta, \tag{16}$$

and one can check that

$$\left.\frac{\partial E_c}{\partial(\theta,\dot{\theta})}\right|_{(0,0)} = \begin{bmatrix} 0 \\ 0 \end{bmatrix},$$

$$\left.\frac{\partial^2 E_c}{\partial(\theta,\dot{\theta})^2}\right|_{(0,0)} = \begin{bmatrix} -hg & 0 \\ 0 & b - a^{-1}h^2r^2 + a\sigma^{-1}\left(1 + a^{-1}hr\right)^2 \end{bmatrix}.$$

Since $-hg < 0$, the Hessian matrix must be negative to stabilize the point $(\theta, \dot{\theta}) = (0, 0)$ which implies that

$$b - a^{-1}h^2r^2 + a\sigma^{-1}\left(1 + a^{-1}hr\right)^2 < 0$$

or equivalently

$$0 > \sigma > -\frac{a\left(1 + a^{-1}hr\right)^2}{b - a^{-1}h^2r^2} \tag{17}$$

where the constant terms are defined in Table 1. □

The asymptotic stability can also be achieved by a suitable choice of a dissipative control. According to the control direction in Eqs. 8 and 9, let the feedback dissipation be $[1, -1]^T u_d$. Then the rate of energy, as in [11], can be computed by

$$\dot{E}_c = -\dot{q}^T M_c M^{-1} \begin{bmatrix} 1 \\ -1 \end{bmatrix} u_d,$$

and choosing

$$u_d = -\dot{q}^T M_c M^{-1} \begin{bmatrix} 1 \\ -1 \end{bmatrix} \tag{18}$$

makes $\dot{E}_c$ positive semi-definite. Now using LaSalle's invariance principle, one may check the asymptotic stability too. So, the complete self-balancing controller is provided by Eqs. 15 and 18 as

$$u_s = k_c u_c + k_d u_d \tag{19}$$

where k_c and k_d are positive values.

Remark 1 In prior work [20], we have examined the performance of the controller provided in this section on a wheeled inverted pendulum whose motion is confined in one dimension (the straight line). In this paper, we consider it as the self-balancing sub-controller of unmanned mobile robots and investigate its performance in conjunction with the robot's motion control in the plane.

Remark 2 Since CL method yields the closed-loop dynamics in Lagrangian form, the total energy (16) available to the mechanism and actuators remains constant or non-increasing, hence the control inputs remain bounded for the fixed stabilizing control gains. Although in this section we assume no specific bounds on the allowable values of the control inputs, i.e., the required inputs are available to the robot, but in the simulation section, the value of the required inputs as well as input saturation is numerically investigated for the control system.

4 Motion Control on Lie Group SE(2)

For the planar motion control, we make use of the Lie group setting of SE(2) to study the stabilization of the robot at an specified posture. For detailed explanation of the exponential coordinates of SE(2) and its time derivative, used in this section, the reader is referred to [19].

Let the nonholonomic constraints (5) be expressed in the left-invariant kinematic control system

$$\dot{g} = g\hat{\xi}\,, \quad g(0) = g_0 \tag{20}$$

with the input $\hat{\xi}$. The configuration $g \in \mathrm{SE}(2)$ and the corresponding Lie algebra element $\hat{\xi} \in \mathfrak{se}(2)$ are denoted by

$$g = \begin{bmatrix} \cos\psi & -\sin\psi & x \\ \sin\psi & \cos\psi & y \\ 0 & 0 & 1 \end{bmatrix}, \quad \hat{\xi} = \begin{bmatrix} 0 & -\dot{\psi} & r\dot{\varphi} \\ \dot{\psi} & 0 & 0 \\ 0 & 0 & 0 \end{bmatrix}.$$

We also parameterize the configuration g by the orientation and position in the space coordinates as $P = [\psi, x, y]^T$ and the input $\hat{\xi}$ by the angular and translational velocities in the body-fixed frame as $\xi = [\dot{\psi}, r\dot{\varphi}, 0]^T$.

Since SE(2) is a matrix Lie group, the exponential map $\exp : \hat{\eta} \in \mathfrak{se}(2) \to \mathrm{SE}(2) \ni g$ coincides with the matrix exponential $g = \exp\hat{\eta}$. The inverse map $\log : g \in \mathrm{SE}(2) \to \mathfrak{se}(2) \ni \hat{\eta}$ exists for $-\pi < \psi < \pi$ which is given by the matrix logarithm as

$$\hat{\eta} = \log_{\mathrm{SE}(2)} g = \begin{bmatrix} \hat{\psi} & A^{-1}(\psi)p \\ 0 & 0 \end{bmatrix} \triangleq \begin{bmatrix} 0 & -\psi & s_x \\ \psi & 0 & s_y \\ 0 & 0 & 0 \end{bmatrix} \tag{21}$$

where

$$A^{-1}(\psi) = \begin{bmatrix} \alpha(\psi) & \psi/2 \\ -\psi/2 & \alpha(\psi) \end{bmatrix}, \quad \alpha(\theta) = (\psi/2)\cot(\psi/2)$$

$p = [x, y]^T$, and $s = [s_x, s_y]^T = A^{-1}(\psi)p$. The term $\hat{\eta} = \log_{\mathrm{SE}(2)} g$ is called the exponential coordinates of g

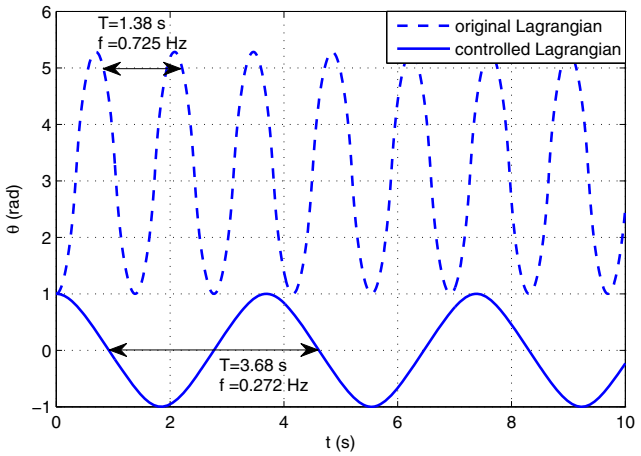

Fig. 2 Changing the stable equilibrium from downward $\theta = \pi$ to upright $\theta = 0$ by controlled Lagrangian

and is parameterized by $\eta = [\psi, s_x, s_y]^T$. Using the exponential coordinates, the control law for steering the robot to the origin with zero attitude is developed in the following proposition.

Proposition 2 *Consider the kinematic system (20) which is controlled with the nonholonomic input*

$$\xi = -\begin{bmatrix} \psi + \kappa\tilde{\psi} \\ s_x \\ 0 \end{bmatrix}, \quad \tilde{\psi} = -\arctan\frac{s_y}{s_x}. \tag{22}$$

There always exists some appropriate choice of the control gain κ for that the control system is asymptotically stabilized around the identity, i.e., $g \to I$ ast $\to \infty$, where $\tilde{\psi} \triangleq 0 \forall s_y = s_x = 0$.

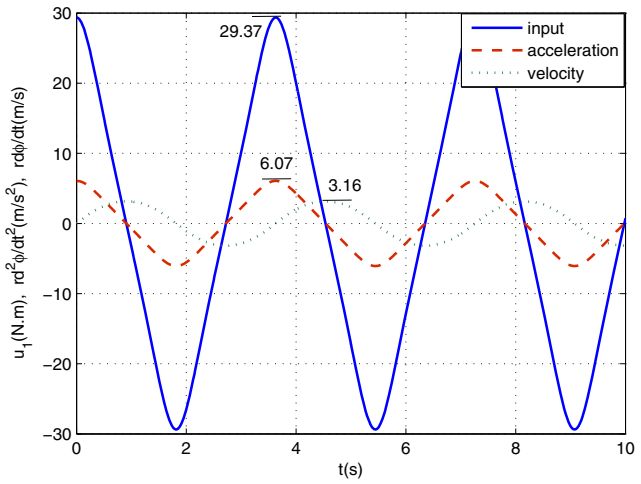

Fig. 3 Control input, translational acceleration and velocity for the controlled Lagrangian dynamics

Table 2 Peak values of undamped free oscillations for the controlled Lagrangian system

Deviation θ(rad)	Max. Input u_1(N.m)	Divergence u_1(N.m)	Max. Accel. $r\ddot{\varphi}(m/s^2)$
2.0	309.8	63.05	53.31
1.0	29.37	25.23	6.07
0.5	12.94	11.85	2.73
0.3	7.58	7.12	1.61
0.1	2.50	2.33	0.53

Proof Suppose that the candidate Lyapunov function has the form

$$\begin{aligned} F(\eta) &= \eta^T \,\mathrm{diag}(\kappa^{-1}, I_2)\eta + (k_F + 1)\tilde{\psi}^2 \\ &= \kappa^{-1}\psi^2 + s^T s + (k_F + 1)\tilde{\psi}^2 \end{aligned} \tag{23}$$

where the constant k_F is a positive scalar. The time derivative of the exponential coordinates for SE(2) can be computed by

$$\dot{\eta} = \begin{bmatrix} 1 & 0 \\ \frac{1}{\psi}(I - A^{-T}(\psi))s & A^{-T}(\psi) \end{bmatrix}\xi \tag{24}$$

where $A^{-T} = (A^{-1})^T$. Replacing ξ with the velocity control (22), it follows that

$$\dot{\eta} = -\begin{bmatrix} (\psi + \kappa\tilde{\psi}) \\ \left(I + \frac{\kappa\tilde{\psi}}{\psi}(I - A^{-T}(\psi)) - A^{-T}(\psi)E_{22}\right)s \end{bmatrix}$$

where $E_{22} \in \mathbb{R}^{2\times 2}$ with one on its (2,2) component and zeros elsewhere. Using the above equation and matrix calculations, one can check that the time derivative of F becomes

$$\dot{F}(\eta) = -2\kappa^{-1}(\psi + k\psi/2)^2 - k_F s^T Q_1(\kappa, \eta, \tilde{\psi})s - s^T Q_2(\kappa, \eta, \tilde{\psi})s \tag{25}$$

where

$$Q_1 = \begin{bmatrix} \frac{\kappa\tilde{\psi}^2}{s^T s} & \frac{\tilde{\psi}\alpha(\psi)}{s^T s} \\ \frac{\tilde{\psi}\alpha(\psi)}{s^T s} & \frac{\tilde{\psi}\psi + \kappa\tilde{\psi}^2}{s^T s} \end{bmatrix},$$

$$Q_2 = \begin{bmatrix} 2 + 2\kappa\tilde{\psi}\frac{1-\alpha(\psi)}{\psi} + \frac{\kappa\tilde{\psi}^2}{2s^T s} & \frac{\psi}{2} + \frac{\tilde{\theta}\alpha(\psi)}{s^T s} \\ \frac{\psi}{2} + \frac{\tilde{\psi}\alpha(\psi)}{s^T s} & 2\left(1 + \frac{\kappa\tilde{\psi}}{\psi}\right)(1 - \alpha(\psi)) + \frac{2\tilde{\psi}\psi + \kappa\tilde{\psi}^2}{2s^T s} \end{bmatrix}.$$

The matrix Q_1 is positive for

$$\kappa^2\tilde{\psi}^2 + \kappa\tilde{\psi}\psi - \alpha^2(\psi) > 0, \text{ or } \kappa > \frac{\pi}{|\tilde{\psi}|} > 2.$$

From the expression of Q_2, there certainly exits a $\tilde{\psi}^*$ such that once $|\tilde{\psi}| < |\tilde{\psi}^*|$ the matrix Q_2 becomes positive definite for

$$\kappa > \frac{\pi}{|\tilde{\psi}^*|} > 2$$

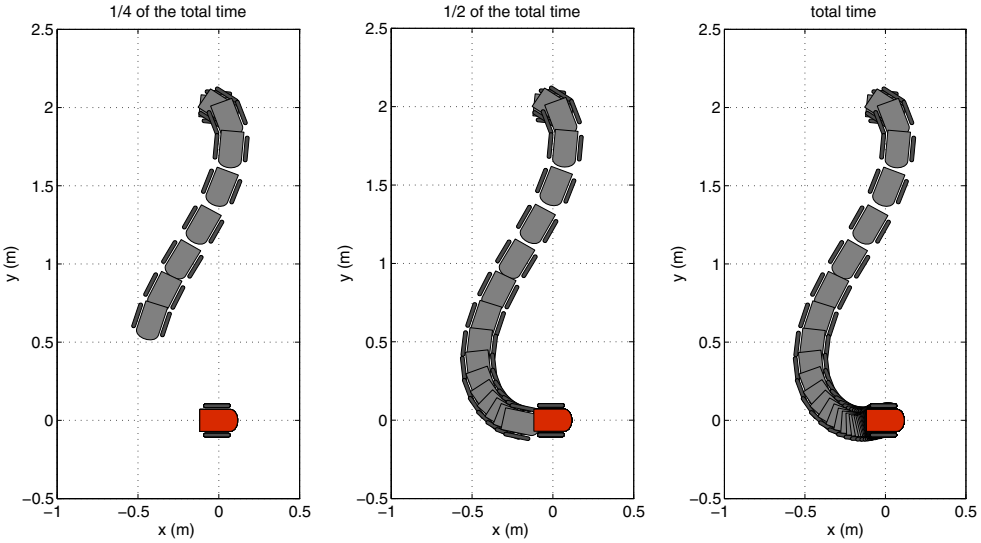

Fig. 4 Parallel parking in the identity in different time zones; the final posture is marked in red color

In order to make the time derivative of F negative definite, there certainly exists a positive scalar $k_F > 0$, such that

$$k_F Q_1 + Q_2 \geq 0, \forall |\tilde{\psi}| \geq |\tilde{\psi}^*|$$

Note that the negative definiteness of $\dot{F}$ for $|\tilde{\psi}| < |\tilde{\psi}^*|$ is already insured by selecting $\kappa > \pi/|\tilde{\psi}^*|$. Therefore $\dot{F}(\eta) < 0$ for $\eta \neq 0$ and the system is asymptotically stabilized at the identity $\hat{\eta} = 0$ (or $g = I$).

For a theoretical consideration on the selection of the control gain κ, set

$$\begin{aligned}\tilde{\psi} &= -\arctan\left(s_y/s_x\right) \\ &= -\arctan\frac{(y/x)-\tan(\psi/2)}{1+(y/x)\tan(\psi/2)} \\ &= \begin{cases} \arctan(y/x)-\psi/2, & (y/x)\tan(\psi/2) > -1 \\ \arctan(y/x)-\psi/2+\pi, & (y/x)>0,\ (y/x)\tan(\psi/2)<-1 \\ \arctan(y/x)-\psi/2-\pi, & (y/x)<0,\ (y/x)\tan(\psi/2)<-1 \end{cases} \end{aligned} \quad (26)$$

When, we confine $\tilde{\psi} \in (-\frac{\pi}{2}, \frac{\pi}{2})$, we can take

$$\tilde{\psi} = \frac{\psi}{2} - \arctan\frac{y}{x}$$

which is always the case when $\tilde{\psi}$ is near 0. Now consider the case that $s_x = 0$ but $g \neq I$ or $\xi = -\begin{bmatrix} \psi + \kappa\tilde{\psi} & s_x & 0 \end{bmatrix}^T \neq 0$ which requires that $\psi + \kappa\tilde{\psi} \neq 0$. For $s_x = 0$ it follows that $1 + (y/x)\tan(\psi/2) = 0$ and

$$\arctan(y/x) = -\arctan(\cot(\psi/2)),$$

thus we get to

$$\kappa > |\psi/\tilde{\psi}| = \psi(\psi/2 + \arctan(\cot(\psi/2)))^{-1} = \frac{2}{\pi}\psi.$$

This again leads to the selection of $\kappa > 2$. □

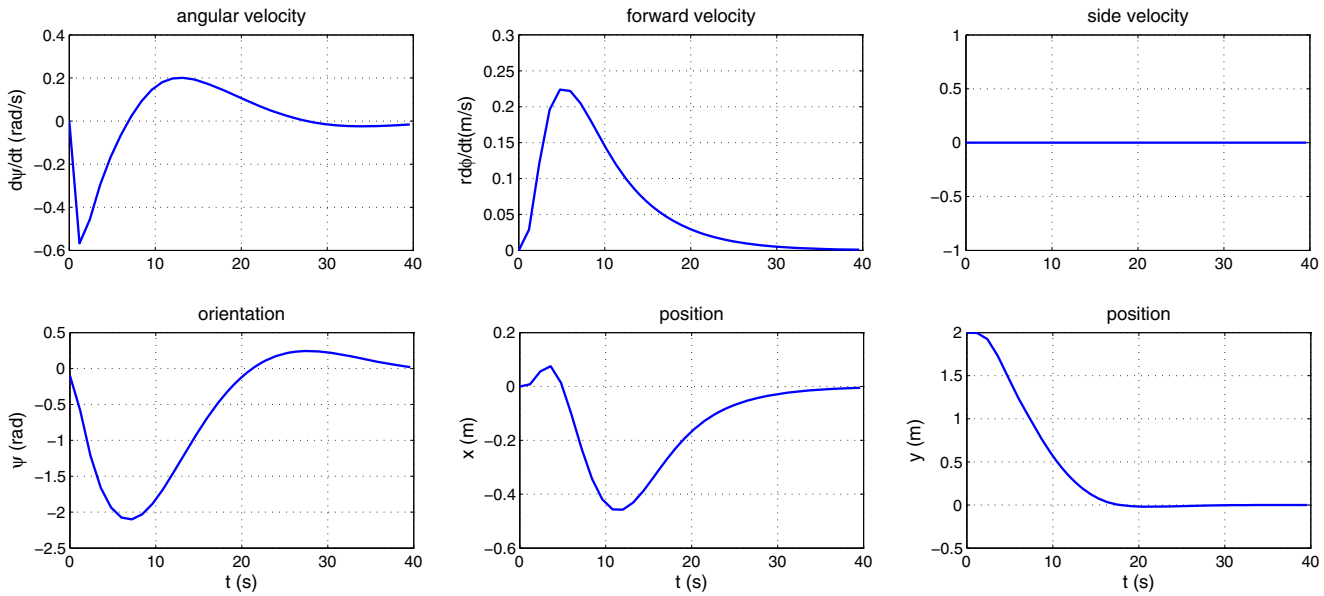

Fig. 5 Components of velocity and configuration during the parallel parking

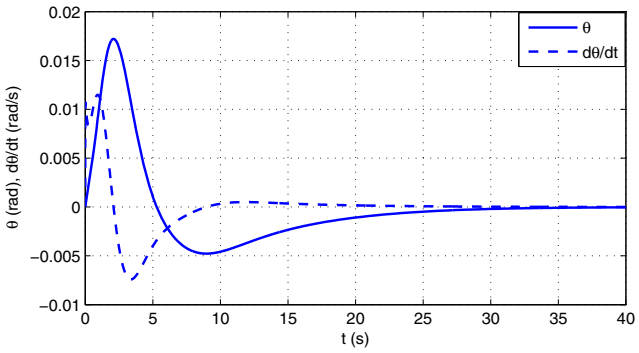

Fig. 6 The self-balancing performance during the parallel parking

The kinematic control (22) can easily be applied to the dynamic system through a backstepping technique. Adapting the block backstepping formula in [21], the system is the cascade connection of the kinematics (20) and the dynamics (3) which we rewrite them as follows

$$\begin{aligned} \dot{P} &= \mathcal{B}\vartheta \\ \dot{\vartheta} &= \mathcal{A}u_b \end{aligned} \tag{27}$$

where

$$\mathcal{B} = \begin{bmatrix} 0 & 1 \\ r\cos\psi & 0 \\ r\sin\psi & 0 \end{bmatrix}, \quad \mathcal{A} = \mathcal{D}\mathcal{M}^{-1}\mathcal{D}^{-1}$$

Taking

$$u_b = \begin{bmatrix} u_{b1} \\ u_{b2} \end{bmatrix} = \mathcal{A}^{-1}\left(\frac{\partial\bar{\xi}}{\partial P}\mathcal{B}\vartheta - \left(\frac{\partial F}{\partial P}\mathcal{B}\right)^T - k_b\left(\vartheta - \bar{\xi}\right)\right) \tag{28}$$

with $k_b > 0$, one can show that the origin is asymptotically stable based on the new Lyapunov function $\bar{F} = F + \frac{1}{2}\left\|\vartheta - \bar{\xi}\right\|^2$. According to proposition 2, the controller for the first-order system is

$$\bar{\xi} = -\begin{bmatrix} s_x \\ \psi + \kappa\tilde{\psi} \end{bmatrix}.$$

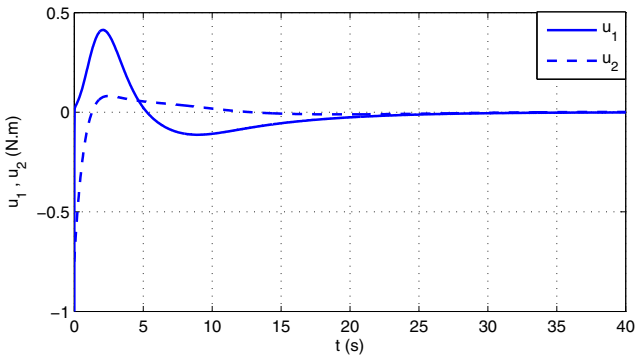

Fig. 7 The control inputs during the parallel parking

5 Dynamic Modeling and Simulation

To evaluate the self-balancing and motion controllers designed in the preceding sections, we develop a unified 5DF dynamic model of the system and then the controllers are imposed by simulation.

5.1 Nonholonomic EL Equations

The body-fixed frame of the wheel and the robot both possess only two rotations in the space coordinates. The two angles can be considered as the two first Euler angles to get to the corresponding rotation matrices. For the robot's body

$$R_\psi = \begin{bmatrix} c\psi & -s\psi & 0 \\ s\psi & c\psi & 0 \\ 0 & 0 & 1 \end{bmatrix}, \; R_\theta = \begin{bmatrix} c\theta & 0 & s\theta \\ 0 & 1 & 0 \\ -s\theta & 0 & c\theta \end{bmatrix}, \; R_b = R_\psi R_\theta = \begin{bmatrix} c\psi c\theta & -s\psi & c\psi s\theta \\ s\psi c\theta & c\psi & s\psi s\theta \\ -s\theta & 0 & c\theta \end{bmatrix}$$

where $c\theta \triangleq \cos\theta$, $s\theta \triangleq \sin\theta$ and so on. The matrix form of the angular velocity in the body-fixed frame can be written by

$$\hat{\omega}_b = {R_b}^T\dot{R}_b = \begin{bmatrix} 0 & -\dot{\psi}c\theta & \dot{\theta} \\ \dot{\psi}c\theta & 0 & \dot{\psi}s\theta \\ -\dot{\theta} & -\dot{\psi}s\theta & 0 \end{bmatrix}$$

or $\omega_b = [-\dot{\psi}s\theta, \dot{\theta}, \dot{\psi}c\theta]^T$. Replacing θ with φ in the above two equations similarly yields the wheel's rotation matrix $R_w = R_\psi R_\varphi$ and its angular velocity $\omega_w = [-\dot{\psi}s\varphi, \dot{\varphi}, \dot{\psi}c\varphi]^T$.

For translational velocities, let the position of the center of mass for the wheel and robot be

$$p_w = \begin{bmatrix} x \\ y \\ r \end{bmatrix}, \quad p_b = p_w + \ell R_b e_1 = \begin{bmatrix} x + \ell c\psi s\theta \\ y + \ell s\psi s\theta \\ r + \ell c\theta \end{bmatrix}$$

Differentiating them gives the velocities as

$$v_w = \begin{bmatrix} \dot{x} \\ \dot{y} \\ 0 \end{bmatrix}, \quad v_b = \begin{bmatrix} \dot{x} - \ell\dot{\psi}s\psi s\theta + \ell\dot{\theta}c\psi c\theta \\ \dot{y} + \ell\dot{\psi}c\psi s\theta + \ell\dot{\theta}s\psi c\theta \\ -\ell\dot{\theta}s\theta \end{bmatrix}.$$

Now the total kinetic energy can be written as

$$\mathbf{T} = \frac{1}{2}\left(m_w v_w^2 + m_b v_w^2 + \omega_w^T\mathbf{J}_w\omega_w + \omega_b^T\mathbf{J}_b\omega_b\right) = \frac{1}{2}\dot{\mathbf{q}}^T\mathbf{M}\dot{\mathbf{q}} \tag{29}$$

where

$$\mathbf{J}_w = \begin{bmatrix} J_{w1} & 0 & 0 \\ 0 & J_{w2} & 0 \\ 0 & 0 & J_{w3} \end{bmatrix}, \quad \mathbf{J}_b = \begin{bmatrix} J_{b1} & 0 & 0 \\ 0 & J_{b2} & 0 \\ 0 & 0 & J_{b3} \end{bmatrix}.$$

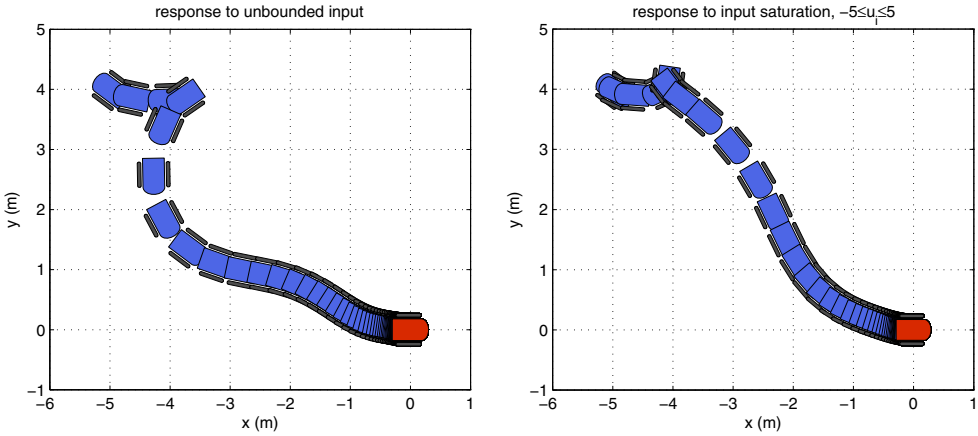

Fig. 8 Switching control from the backward to the forward motion; the final posture is marked in red color

Since the motion is in the plane and the moment of inertia about e_1 is not noticeable, for simplification, we assume it as that of e_3. The mass-inertia matrix in (29) is now

$$\mathbf{M} = \begin{bmatrix} m & 0 & -hs\psi s\theta & 0 & hc\psi c\theta \\ 0 & m & hc\psi s\theta & 0 & hs\psi c\theta \\ -hs\psi s\theta & hc\psi s\theta & J + h\ell s^2\theta & 0 & 0 \\ 0 & 0 & 0 & J_{w2} & 0 \\ hc\psi c\theta & hs\psi c\theta & 0 & 0 & b \end{bmatrix}.$$

The Coriolis and centripetal forces are given by

$$C(\mathbf{q}, \dot{\mathbf{q}})\,\dot{\mathbf{q}} = \dot{\mathbf{M}}(\mathbf{q})\,\dot{\mathbf{q}} - \frac{\partial \mathbf{T}}{\partial \mathbf{q}};$$

$$C(\mathbf{q}, \dot{\mathbf{q}}) = \begin{bmatrix} 0 & 0 & -h\left(\dot{\psi}c\psi s\theta + \dot{\theta}s\psi c\theta\right) & 0 & -h\left(\dot{\psi}s\psi c\theta + \dot{\theta}c\psi s\theta\right) \\ 0 & 0 & h\left(\dot{\theta}c\psi c\theta - \dot{\psi}s\psi s\theta\right) & 0 & h\left(\dot{\psi}c\psi c\theta - \dot{\theta}s\psi s\theta\right) \\ 0 & 0 & 2h\ell\dot{\theta}c\theta s\theta & 0 & 0 \\ 0 & 0 & 0 & 0 & 0 \\ 0 & 0 & -\frac{1}{2}h\ell\dot{\psi}c\theta s\theta & 0 & 0 \end{bmatrix}.$$

Using Lagrange multipliers the dynamics of the system satisfies the following constrained Euler-Lagrange equations

$$\bar{\mathbf{M}}(\mathbf{q})\,\dot{\zeta} + \bar{C}(\mathbf{q}, \zeta)\,\zeta + d\bar{V}(\mathbf{q}) = \bar{B}(\mathbf{q}, \zeta)\,u(t) \tag{30}$$

where $\zeta = [\dot{\psi}, \dot{\varphi}, \dot{\theta}]^T$,

$$\bar{\mathbf{M}} = G^T\mathbf{M}G = \begin{bmatrix} J + h\ell s^2\theta & 0 & 0 \\ 0 & a & hrc\theta \\ 0 & hrc\theta & b \end{bmatrix},$$

$$\bar{C}(\mathbf{q}, \dot{\mathbf{q}}) = G^T\mathbf{M}\dot{G} + G^TCG = \begin{bmatrix} 2h\ell\dot{\theta}c\theta s\theta & hr\dot{\psi}s\theta & 0 \\ -hr\dot{\psi}s\theta & 0 & -hr\dot{\theta}s\theta \\ -h\ell\dot{\psi}c\theta s\theta & 0 & 0 \end{bmatrix},$$

and $G = [f_1, f_2, f_3]$ is the constraint matrix in the kinematic model (6). The control and the gravity terms are

$$d\bar{V} = \begin{bmatrix} 0 \\ 0 \\ -hgs\theta \end{bmatrix}, \quad \bar{B}u = \begin{bmatrix} 1 & 0 \\ 0 & 1 \\ 0 & -1 \end{bmatrix} \begin{bmatrix} u_2 \\ u_1 \end{bmatrix}.$$

Substituting all the terms into Eq. 30 yields the EL equations as

$$\begin{aligned} &(J + h\ell\sin^2\theta)\ddot{\psi} + 2h\ell\dot{\psi}\dot{\theta}\cos\theta\sin\theta + hr\dot{\psi}\dot{\varphi}\sin\theta = u_2 \\ &a\ddot{\varphi} + hr\ddot{\theta}\cos\theta - hr\sin\theta(\dot{\psi}^2 + \dot{\theta}^2) = u_1 \\ &b\ddot{\theta} + hr\ddot{\varphi}\cos\theta - h\ell\dot{\psi}^2\cos\theta\sin\theta - hg\sin\theta = -u_1 \end{aligned} \tag{31}$$

This dynamic model along with the kinematics (20) provides the complete set of 5DF equations of the planar motion for the self-balancing robot.

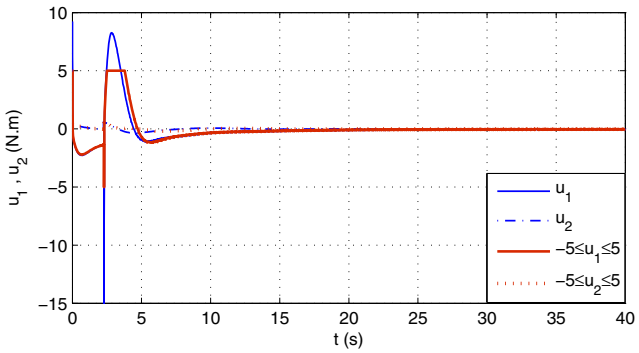

Fig. 9 Control inputs corresponding to the robot's motion in Fig. 8

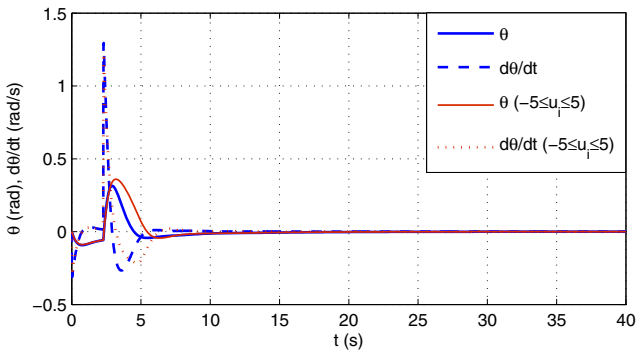

Fig. 10 Self-balancing behavior of the robot during the motion shown in Fig. 8

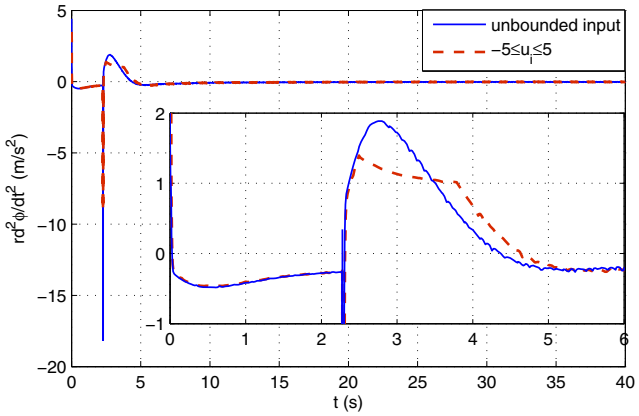

Fig. 11 Robot's acceleration for both the bounded and unbounded inputs

5.2 Numerical simulations and discussion

For simulation, set the robot parameters be

$$m_w = 3.5,\ m_b = 15\,(\text{kg}),\ J_{w2} = 0.15,\ J_{w3} = 0.1,\ J_{b2} = 0.45,\ J_{b3} = 0.3\,(\text{kg.m}^2),$$
$$l = 0.2,\ \ell = 0.3,\ r = 0.2\,(\text{m}).$$

Regarding the conditions in propositions 1 and 2, we select the control parameters as

$$\sigma = -0.2,\ \kappa = 5,\ k_d = 0.8,\ k_c = 10,\ k_b = 10,\ k_F = 100$$

We first evaluate the performance of the self-balancing controller (15) individually. For this, we set all the initial conditions zero but $\theta_0 = 1$ rad and simulate the dynamic model (31) for the open-loop case with $u_1 = u_2 = 0$ as well as the closed-loop case with $u_1 = u_c, u_2 = 0$. The simulation result for the pitch angle, the angle of the robot's body with respect to the vertical, for the both uncontrolled and controlled cases are compared in Fig. 2. Changing the stable equilibrium of the robot's body from the downward $\theta = \pi$ to the upright $\theta = 0$ is evident. Such a wide region of attraction from the upright shows the nonlinear performance of the controller too. Moreover, these undamped free oscillations enable us to observe some other dynamic properties of the modified Lagrangian system, for instance the natural frequency, and to examine how those properties vary with different selections of the CL constant σ. The control input as well as the translational velocity and acceleration of the robot corresponding to these free oscillations are shown in Fig. 3. One can observe the peak values of the input, velocity and acceleration for the specific selection of the CL gains and initial conditions.

In Table 2, we list the peak values for some other initial deviations of the robot's body from the upright. The data in the third column represents the input saturation value for which the system starts to diverge. First observation is that the CL system is able to bring up the robot's body even form $\theta_0 = 2 > \pi/2$ and makes it stable at the upright. Second, the more the robot's body get deviated from the upright the more control torque is required to bring it back to the upright. Third, collecting such data in the design process enables us to select proper actuators for the real robot. Note that these maximum input values for the undamped dynamics would definitely ensure enough torque for asymptotic stability of the dissipative control system too.

Now, we apply the both controllers to investigate the posture stabilization of the self-balanced robot. For this, set the inputs in Eq. 31 as

$$u_1 = u_s + u_{b1},\ \ u_2 = u_{b2}$$

where u_s, given by Eq. 19, asymptotically stabilizes the robot at the upright and u_b, given by Eq. 28, parks the robot in the origin with zero attitude. Set the initial posture be $P_0 = [\psi, x, y]_0^T = [0, 0, 2]^T$ which is parallel to the identity. Figure 4 shows the simulated trajectory with attitude for 40 s in which the robot drives to the origin and its orientation converges to zero. The components of the body velocity, position, and orientation are illustrated in Fig. 5. Preserving the nonholonomic constraint or zero side-velocity is also

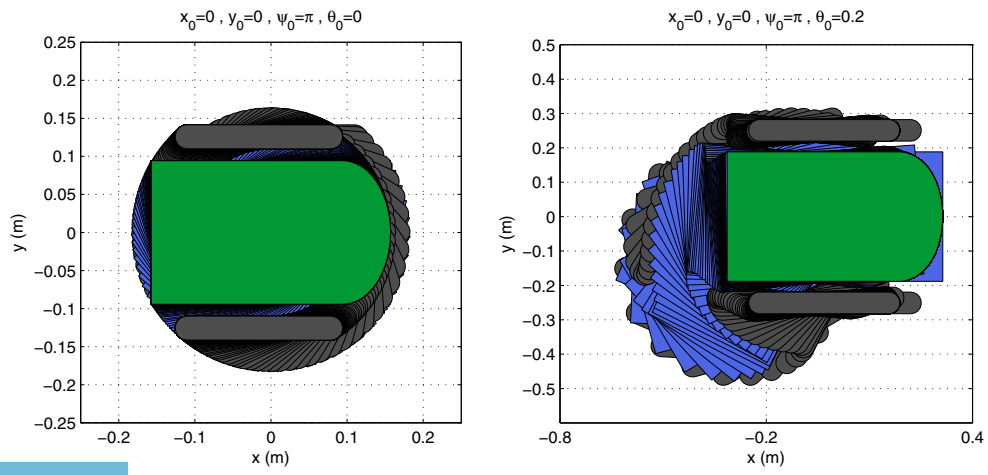

Fig. 12 Attitude stabilization for the robot initiated at the origin; the final posture is marked in green color

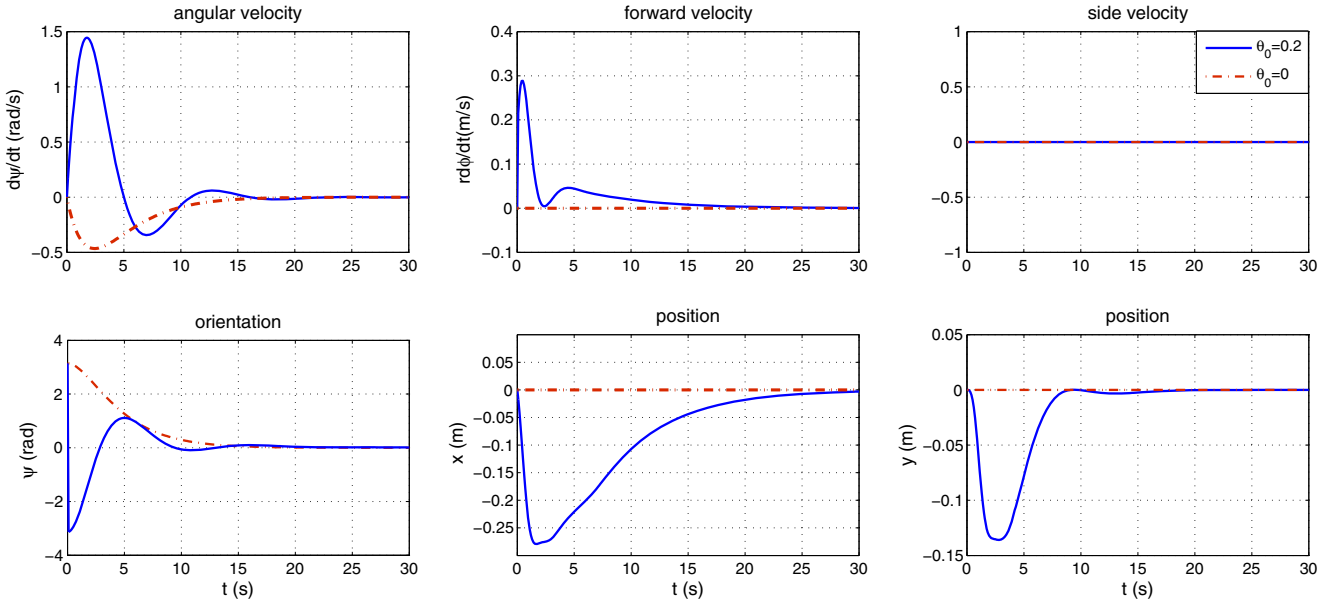

Fig. 13 The components of velocity and configuration during the attitude stabilization

evident in this picture. The robot's angle with respect to the vertical and its time derivative are illustrated in Fig. 6. The self-balancing performance during the planar motion is also evident in this picture. Figure 7 shows the time evolution of the control inputs for this motion.

The other case we are interested in is the switching control between the backward and forward motions. For this, set the initial posture be $P_0 = [\psi, x, y]_0^T = [2.5, -5, 4]^T$. The robot's trajectory with attitude is simulated for 40 s and illustrated in Fig. 8. The planar motion in presence of the input saturation, $-5 \leq u_i \leq 5 \forall i = 1, 2$, is also simulated in this figure. The performance of the planar motion controller for steering the system to the origin is evident. Both the unbounded and bounded control inputs are shown in Fig. 9. The robot's attitude with respect to the vertical and its time derivative are depicted in Fig. 10. One can observe by simulation that the settling time is about 1 s longer for the case with the bounded inputs, however the robot's body does not diverge from the upright. We can see in this figure that the deviation about 0.3 rad occurs in θ at time around 3 s and is compensated by the input with the upper bound 5 N.m which is even lower than the diverging value 7.12 N.m in Table 2 for the free oscillations. This result again shows that the control actuators can be selected based on those required inputs in the table.

Figure 11 shows the translational acceleration of the robot for the both motions simulated in Fig. 8. In spite of assuming no bound on the robot's acceleration in the planar motion, the performance of the self-balancing nonlinear

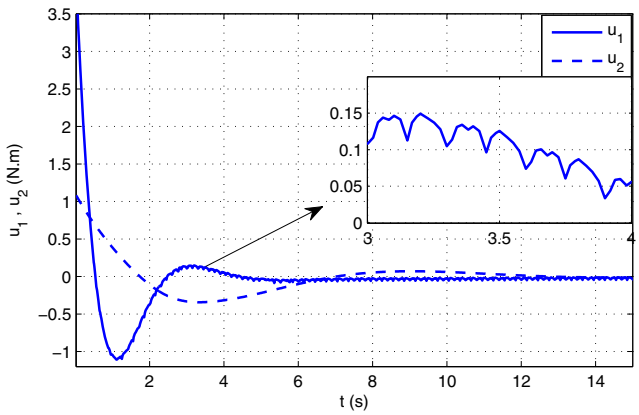

Fig. 14 The control inputs for the case of $\theta_0 = 0.2$

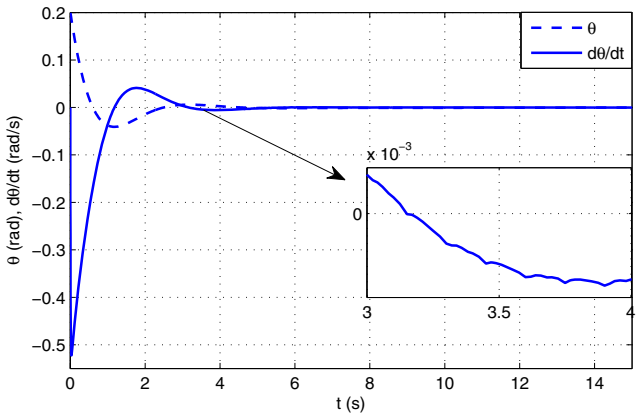

Fig. 15 The self-balancing behavior of the robot for the case of $\theta_0 = 0.2$

controller is evident in compensating any wide deviations from the upright. However, one may use the Eq. 4 which provides a direct correspondence between the motion control input u_b and the robot's angular and translational accelerations $\ddot{\psi}$, $r\ddot{\varphi}$ to further investigate the planar motion control with bounded accelerations. The planar velocity and acceleration can also vary somewhat according to the proportional and dissipation gains κ, k_b in the motion control law. The acceleration due to the controlled Lagrangian dynamics is already discussed in Table 2 and Fig. 3.

Finally, we consider two other critical cases for which the robot initiated at the origin with a non-zero attitude. For this, set $P_0 = [\psi, x, y]_0^T = [\pi, 0, 0]^T$. Figure 12 (left) shows that the attitude is stabilized by a pure rotational motion whenever the robot's body remains at the upright. Now, let the initial deviation of the robot's body from the vertical be non-zero, for instance $\theta_0 = 0.2$ rad. The attitude stabilization for $t = 30$ s is shown in Fig. 12 (right). Note that for the self-balancing control, the robot's position has to oscillate around the origin in the process of the attitude stabilization, but it again converges to the origin as time tends to infinity. The velocity and configuration of the robot for these two cases are compared in Fig. 13. The control inputs and the self-balancing behavior of the robot for the case of $\theta_0 = 0.2$ rad are respectively illustrated in Figs. 14 and 15.

6 Conclusion

While geometric and Lie group methods have been well studied in theory and extensively applied to holonomic systems, their extension to nonholonomic systems and practical applications is still an active field of research. In this paper, two classes of geometric controllers are applied for self-balancing and posture stabilization of unmanned mobile robots. The logarithmic motion control can accomplish the limitations due to the singularities and discontinuities which occasionally happen in the controllers developed for nonholonomic systems. This control, which stabilizes both the position and orientation of the robot, can also be applied to a wide variety of unicycle-type vehicles. Since the method of controlled Lagrangian modifies the dynamic structure of the system and nonlinearly change the stable equilibrium, it is a powerful approach for balancing the internal dynamics of the systems which are inherently unstable whereas they must achieve other control tasks at the same time. The other controllers developed in the literature for the motion control of mobile robots in conjunction with the CL controller designed in this paper are expected to be applicable to self-balancing mobile robots. A comprehensive dynamic model is developed without simplifications to make it as close to the real robot's dynamics as possible for this step. The excellent performance of the proposed controllers in the numerical simulations is a guiding significance to investigating them experimentally on real-world applications in the next step.

Acknowledgements This work is supported by National Natural Science Foundation (NNSF) of China under Grant 61374033. The authors would also like to thank the reviewers for the valuable comments.

References

1. Chan, R.P., Stol, K.A., Halkyard, C.R.: Review of modelling and control of two-wheeled robots. Ann. Rev. Control **37**, 89–103 (2013)
2. Huang, C.: The development of self-balancing controller for one-wheeled vehicles. Engineering **2**, 212–219 (2010)
3. Lee, J.H., Shin, H.J., Lee, S.J., Jung, S.: Balancing control of a single-wheel inverted pendulum system using air blowers. Mechatronics **23**, 926–932 (2013)
4. Han, S.I., Lee, J.M.: Balancing and velocity control of a unicycle robot based on the dynamic model. IEEE Tran. Ind. Electron. **62**, 405–413 (2015)
5. Pinto, L.J., Kim, D.H., Lee, J.Y.: Development of a Segway robot for an intelligent transport system. IEEE/SICE Int. Symposium on System Integration, Fukuoka (2012)
6. Raffo, G.V., Ortega, M.G., Madero, V., Rubio, F.R.: Two-wheeled self-balanced pendulum workspace improvement via underactuated robust nonlinear control. Control Eng. Pract. **44**, 231–242 (2015)
7. Bature, A.A., Buyamin, S.: A comparison of controllers for balancing two wheeled inverted pendulum robot. Mechatronics **14**, 62–68 (2014)
8. Pathak, K., Franch, J.: Velocity and position control of a wheeled inverted pendulum by partial feedback linearization. IEEE Tran. Robot. **21**, 505–513 (2005)
9. Lin, S., Tsai, C., Huang, H.: Adaptive robust self-balancing and steering of a two-wheeled human transportation vehicle. J. Intell. Robot. Syst. **62**, 103–123 (2011)
10. Bloch, A.M., Leonard, N.E., Marsden, J.E.: Controlled Lagrangians and the stabilization of mechanical systems I: the first matching theorem. IEEE Trans. Autom. Control **45**, 2253–2270 (2000)
11. Woolsey, C.A., Reddy, C.K.: Controlled Lagrangian systems with gyroscopic forcing and dissipation. Eur. J. Control **10**(5), 478–496 (2004)
12. Chang, D.E.: The method of controlled Lagrangian systems: Energy plus force shaping. SIAM J. Control Optim. **48**(8), 4821–4845 (2010)
13. Brockett, R.: Asymptotic stability and feedback stabilization. In: Brockett, R.W., Millman, R.S., Sussmann, H.J. (eds.) Differential Geometric Control Theory, pp. 181–191. Birkhauser, Verlag (1983)
14. Serrano, M.E., Godoy, S.A., Quintero, L., Scaglia, G.J.E.: Interpolation based controller for trajectory tracking in mobile robots. J. Intell. Robot. Syst. **86**, 569–581 (2017)
15. Morin, P., Samson, C.: Control of nonholonomic mobile robots based on the transverse function approach. IEEE Trans. Robot. **25**, 1058–1073 (2009)
16. Oriolo, G., Luca, A.D., Vendittelli, M.: WMR control via dynamic feedback linearization: design, implementation, and experimental validation. IEEE Tran. Control Syst. Tech. **10**, 835–852 (2002)

17. Paskonka, J.: Different kinematic path following controllers for a wheeled mobile robot of (2,0) type. J. Intell. Robot. Syst. **77**, 481–498 (2015)
18. Maithripala, D.S., Dayawansa, W.P.: Almost-global tracking of simple mechanical systems on a general class of Lie groups. IEEE Trans. Autom. Control **51**, 216–225 (2006)
19. Bullo, F., Murray, R.: Proportional derivative (PD) control on the Euclidean group. In: European Control Conference, pp. 1091–1097, Rome (1995)
20. Tayefi, M., Geng, Z.: A constructive self-balancing controlled Lagrangian for wheeled inverted pendulum. Chinese Control and Decision Conference, Yinchuan (2016)
21. Khalil, H.K. Nonlinear systems, 3rd edn., pp. 589-603. Prentice Hall, Upper Saddle River (2002)

Morteza Tayefi received the Ph.D. degree in Dynamical Systems and Control from the Department of Mechanics and Engineering Science, Peking University, Beijing, China, in 2017. His current research interests include Stabilisation and Tracking for Underactuated and Nonholonomic Mechanical Systems, Cooperative Control, and Geometric Control Methods.

Zhiyong Geng received the Ph.D. degree in Control Theory and Operational Research from Institute of Systems Science, Chinese Academy of Science, Beijing, China, in 1995. He is currently a Professor at the State Key Laboratory for Turbulence and Complex Systems and a Professor at the Department of Mechanics and Engineering Science, Peking University. His research interest covers Robust Control and Nonlinear Control.